

# Synthesis and Crystal Growth of $Sb_2S_3$ Nanorods Using Iodine as an Initiator Material via Electrochemical Mechanism in Hydrothermal Condition

A. Alemi\*, Y. Hanifehpour Firouzsalar

Department of Inorganic Chemistry, Faculty of Chemistry, University of Tabriz, I. R. Iran

(\* Corresponding author: alemi.aa@gmail.com

(Received: 15 Dec. 2011 and Accepted: 25 Feb. 2012)

## Abstract:

Crystalline antimony sulfide ( $Sb_2S_3$ ) with nanorods morphology was successfully prepared via hydrothermal method by the reaction of elemental sulfur, antimony and iodine as starting materials with high yield at  $180^\circ C$  for 24h. Using oxidation reagents like iodine as an initiator of redox reaction to prepare  $Sb_2S_3$  is reported for first time. Crystal growth of  $Sb_2S_3$  was done by increasing reaction time up to 3 days. The powder X-ray diffraction pattern shows the  $Sb_2S_3$  crystals belong to the orthorhombic phase with calculated lattice parameters of  $a=1.120nm$ ,  $b=1.128nm$  and  $c=0.383nm$ . The quantification of energy dispersive X-ray spectrometry analysis peaks give an atomic ratio of 2:3 for Sb:S. Scanning electron microscopy (SEM) images show that the diameter of nanorods was around 250-380 nm and their length was less than 3  $\mu m$ , respectively. After crystal growth due to increasing the reaction time, diameter of nanorods was reached to about 500-700 nm and their length extended to about 6  $\mu m$ . UV-Vis analysis and emission spectra indicates that band gap of  $Sb_2S_3$  is around 2.82eV, indicating a considerable blue shift relative to the bulk. Moreover, formation mechanism of  $Sb_2S_3$  nano structure was proposed and the effect of reaction time on the growth of nano materials was also investigated.

**Keywords:** Antimony sulfide, Nanorods, Crystal growth, Red-ox reaction, Hydrothermal.

## 1. INTRODUCTION

Antimony sulfide, a layer-structured direct band gap semiconductor with orthorhombic crystal structure, is an important semiconductor with high photo sensitivity and high thermoelectric power [1]. In the past few years, main group metal chalcogenides such as  $A_2B_3$  (where A=As,Sb,Bi and B=S,Se,Te) as significant semiconductors have received ever increasing attention[2]. Due to its good photo conductivity,  $Sb_2S_3$  has received significant attention for potential application in solar energy conversion [3]. It has also been used

in switching devices [4], thermoelectric cooling technologies, optoelectronics in the IR region [5-6], and microwave devices [7], television cameras [8].  $Sb_2S_3$  exist in two forms: orange amorphous phase and black orthorhombic modification with a ribbon like polymeric structure along the [001] direction as the building blocks [9]. Each Sb atom and each S atom is bond to three atoms of the opposite kind within the ribbon-like polymeric structure, forming interlocking  $SbS_3$  and  $SSb_3$  pyramids.

Consequently, amorphous  $Sb_2S_3$  tends to crystallize into one dimensional shape to support the stronger

intrachain covalent bonds over the relatively weak secondary interchain interaction, during the period of crystallization and lattice arrangement, as what found in chain-structured trigonal selenium [10]. Over the past two decades, many methods have been employed to prepare  $Sb_2S_3$ , including thermal decomposition [11], solvothermal reaction [12-13], microwave irradiation [14], vacuum evaporation [3], and other chemical reaction approaches. Besides an elemental reaction,  $Sb_2S_3$  can be prepared by chemical routes, such as sodium thiosulfate and thioacetamide, ammonium sulfide, thiourea, as well as with complex agents in aqueous or non-aqueous solution. Li *et al.* [15] have reported a hydrothermal growth of  $Sb_2S_3$  nanorods without the existence of catalysts or templates. In recent years, solvothermal method has been applied to synthesize  $Sb_2S_3$  nanoparticles, nanorods and micro-tubular  $Sb_2S_3$  crystals. Polygonal bulk tubular  $Sb_2E_3$  ( $E=S, Se$ ) crystals and stibnite nanorods were prepared via the solvothermal route by Zheng *et al.* [16] and Qianet

*et al.* [17], respectively. However, in these methods, the reaction temperature was usually high and the products were usually impure. Therefore, the development of facile, mild and effective methods for creating novel architectures based on nanorods/sub micrometer size rods or nano particles still remains a great challenge. Recently, there is a strong trend towards the application of solution chemical synthesis techniques of materials preparation, in which the particle size and distribution, phase homogeneity and morphology of materials could be well controlled [18]. In this study,  $Sb_2S_3$  nanorods were prepared via hydrothermal method by using antimony, sulfur and iodine in elemental form as raw materials. This is a new route for preparation of  $Sb_2S_3$  nano materials. Elemental iodine is an oxidizing irritant and act as an initiator material in reacting of elemental antimony and sulfur. Without iodine, no reaction is occurred. Using oxidation reagent like iodine as an initiator of red-ox reaction to prepare  $Sb_2S_3$  is reported for first time.

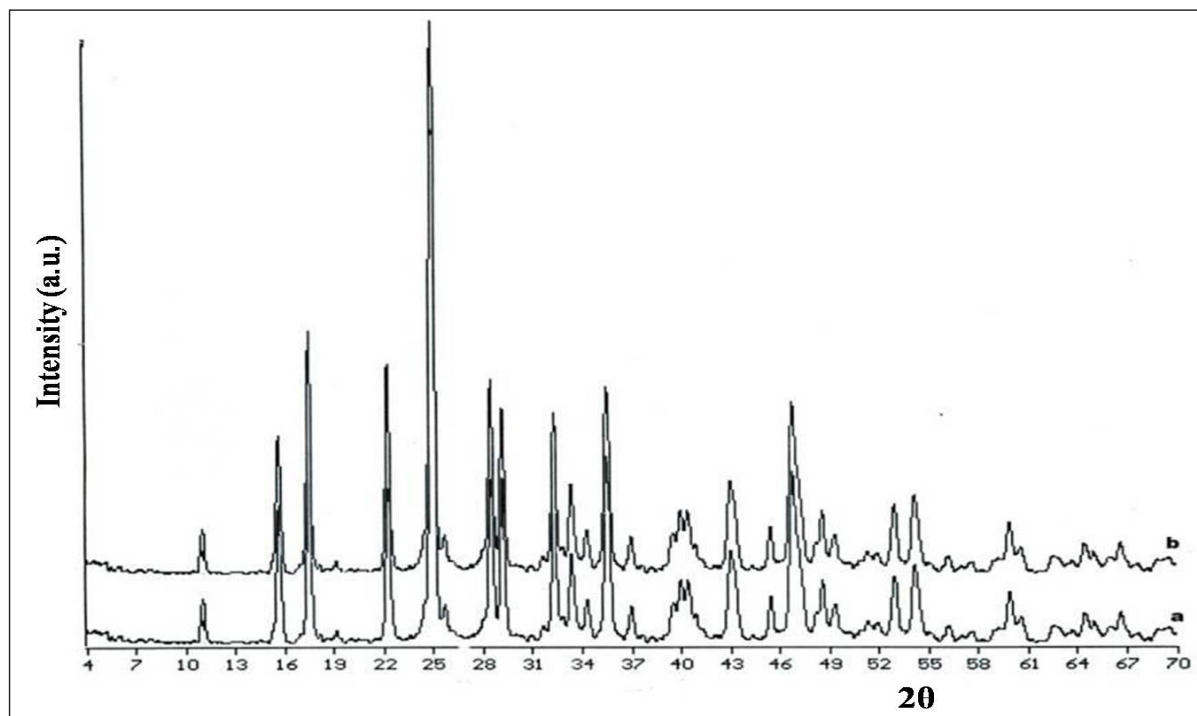


**Figure 1:** XRD patterns of the products obtained under hydrothermal condition at 180°C for 12h (a) and after growth at 180°C for 72h (b).

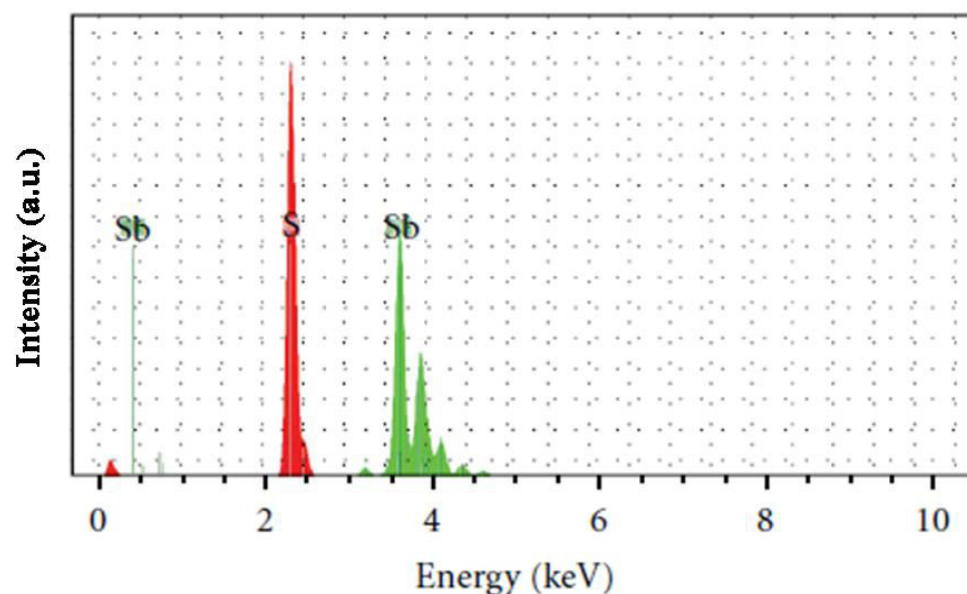


**Figure 2:** EDX patterns of the products obtained under hydrothermal condition at 180°C for 24h.

## 2. EXPERIMENTAL

### 2.1. Synthesis of $Sb_2S_3$ nanorods

All the reagents were of analytical grade and were used without further purification. In a typical procedure, 2 mmol Sb, 3 mmol S and 1mmol  $I_2$  were added to 50 ml distilled water and stirred well for 20 min at room temperature. Then, the mixture was transferred into a 100 ml Teflon-lined autoclave. The autoclave was sealed, maintained at 180°C for 24 h and then cooled at room temperature, naturally. The black precipitate was filtered and washed with dilute chloride acid and water. Finally, the obtained sample was dried at room temperature and used for characterization. Crystal growth of  $Sb_2S_3$  nanorods was done by placing autoclave at 180°C for 72 hour. The crystal structure of the product was characterized by X-ray diffraction (XRD D500 Simens) with  $CuK\alpha$  radiation source ( $\lambda=1.5418 \text{ \AA}$ ). The morphology of materials were examined by a scanning electron microscope (SEM, Leo440i). Elemental analysis was carried

out using a linked ISIS-300, Oxford EDS (energy dispersion spectroscopy detector).

## 3. RESULTS AND DISCUSSION

Figure 1 shows the XRD pattern of the as-prepared  $Sb_2S_3$  before (1.a) and after crystal growth (1.b). All the peaks in the pattern can be indexed to an orthorhombic phase with lattice parameters  $a=1.122 \text{ nm}$ ,  $b=1.128 \text{ nm}$  and  $c=0.384 \text{ nm}$ . The intensity and positions of the peaks are in good agreement with the values reported in the literature (JCPDS card File:42-1393). No characteristic peaks are observed for other impurities such as antimony oxides or  $SbOCl$ . In order to further confirm the chemical compositions of these nano materials, elemental composition analysis was performed by EDXS. Figure 2 shows a typical EDXA spectrum recorded on single crystals, whose peaks are assigned to Sb and S. The atom ratio of Sb and S are 2:3 according to EDXA. This data indicate that we have obtained pure  $Sb_2S_3$

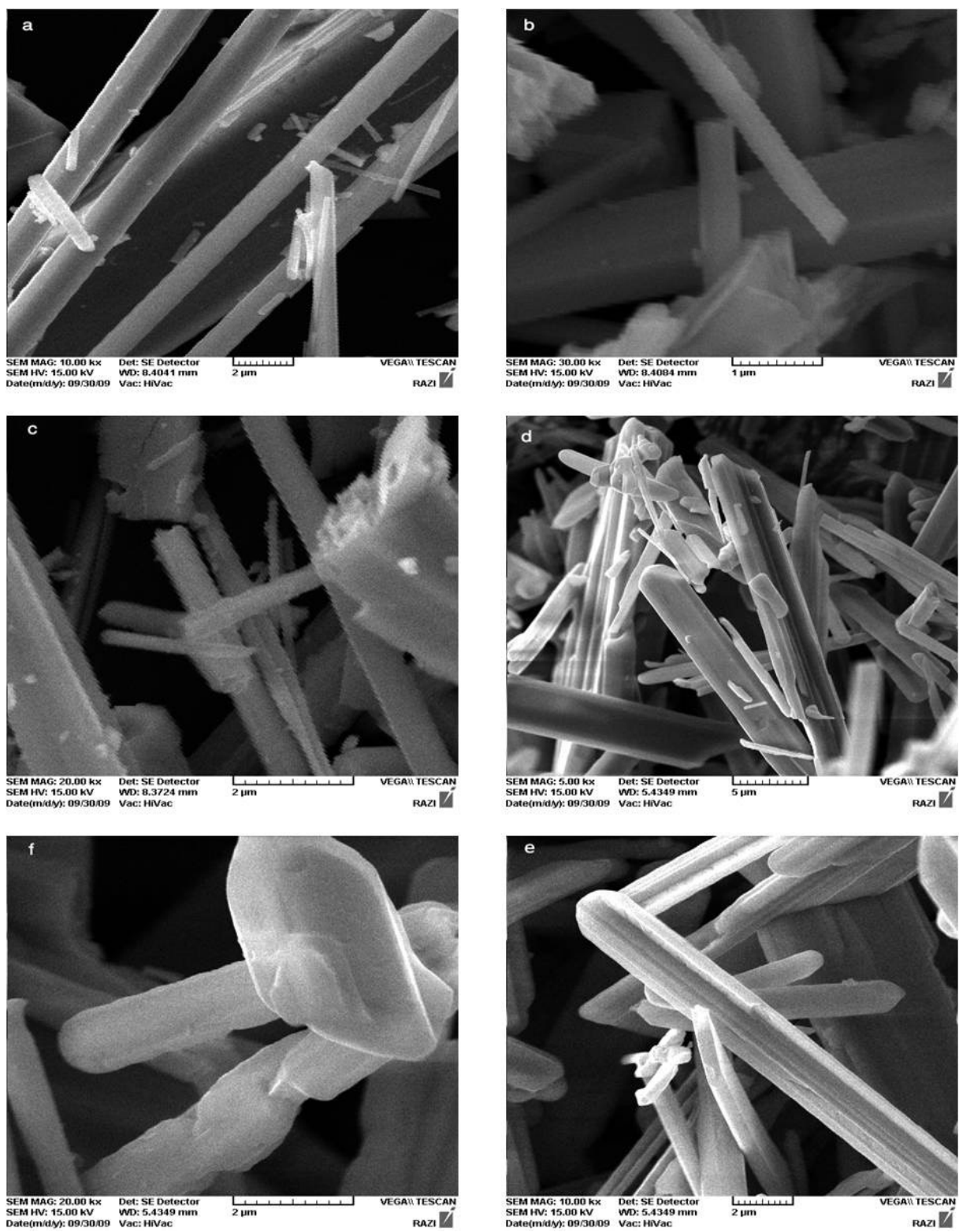


*Figure 3: (a, b, c) SEM image of the  $Sb_2S_3$  nanorods synthesized at 180°C and 24h & figure 3.d, e, f) SEM images of crystal growth of  $Sb_2S_3$  nanorods synthesized at 180°C and 72h.*

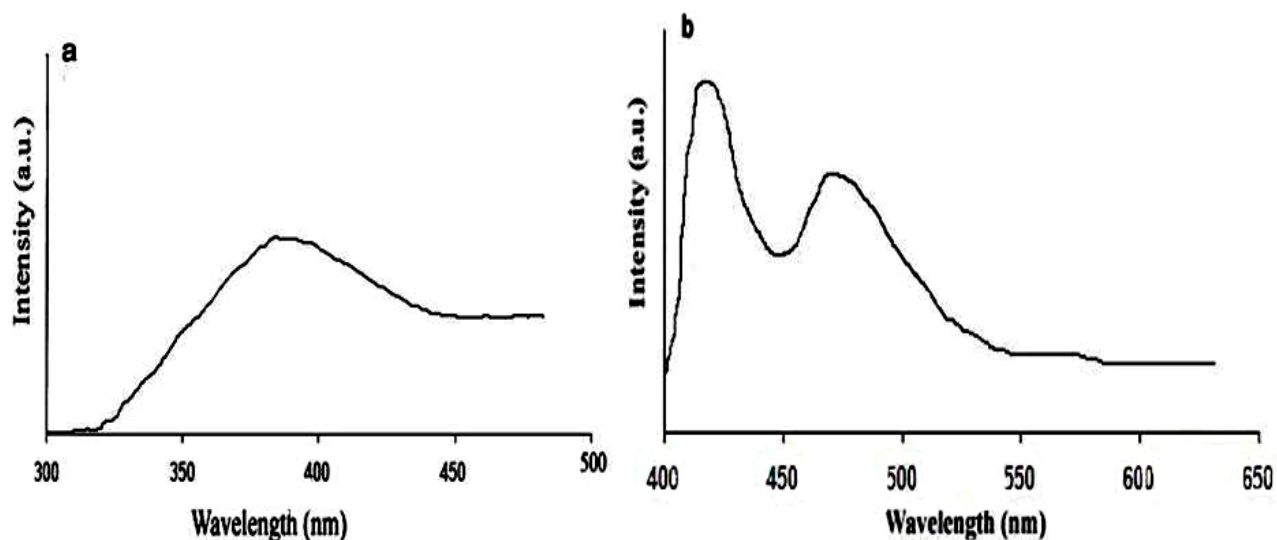


Figure 4: a) excitation spectra b) emission spectra of the products at 180°C and 24h.

single crystals. The morphology of as-prepared  $Sb_2S_3$  at 180°C and 24h was examined by SEM which indicates that the length of nanorods is up to 3  $\mu m$  and their diameters are in the range of 250-380 nm (Figure 3a, b and c). Crystal growth was achieved by increasing the time of the reaction to 72h. Following the crystal growth; the length of rods reached up to 6  $\mu m$  and their diameter to 500-700 nm, respectively (Figure 3d, e and f). To explain the synthesis process, possible chemical reaction involved in the synthesis of  $Sb_2S_3$  could be assigned to iodine and antimony standard electrode potential values. Considering the values of standard electrode potentials of  $Sb^{3+}/Sb$  ( $E_0=0.20$ ) and  $I_2/I^-$  ( $E_0=0.54$ ), the oxidation reaction between Sb and  $I_2$  is possible.



In terms of electrochemistry, since difference of cathodic and anodic standard electrode potentials values is positive, this red-ox reaction can be

occurred. In aqueous solution Iodine and  $I^-$  form complex of  $I_3^-$  that dissolved in water and make a yellowish solution. The existence of  $I^-$  was examined by the forming of red precipitate of  $Hg_2I_2$ .

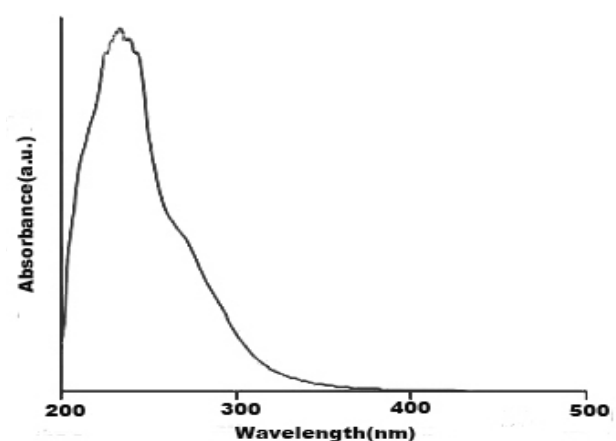
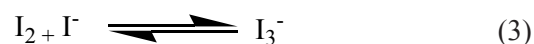
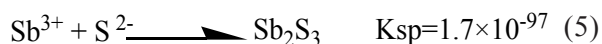


Figure 5: UV/Vis spectra of  $Sb_2S_3$  nanorods synthesized at 180 °C and 24h.

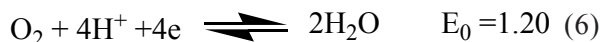
Disproportion of sulfur in this solution is another possibility. Besides the nature of sulfur, the temperature and pressure of autoclave help the disproportion of sulfur.



As the precipitate of  $\text{Sb}_2\text{S}_3$  has a great stability ( $K_{sp}=1.7 \times 10^{-97}$ ), the black precipitate of  $\text{Sb}_2\text{S}_3$  is formed as soon as  $\text{S}^{2-}$  produced. Adding  $\text{Ba}^{2+}$  to the above solution results in white precipitation of  $\text{BaSO}_4$ .



With regard to Oxygen standard electrode potential, if the difference of cathodic and anodic standard electrode potential values is negative, then getting the electron from it to form  $\text{S}^{2-}$  is impossible.



During the precipitation of  $\text{Sb}_2\text{S}_3$ , the conditional electrode potential equals to  $E_0' = E_0 + 0.06 \text{ Pk}_{sp}$  and therefore reaction of  $\text{Sb}^{3+}$  and  $\text{S}^{2-}$  is done with high rate rather than the primary one. As  $\text{Sb}_2\text{S}_3$  is a narrow band gap semiconductor ( $E_g$  is 1.7 eV for bulk), with decreasing in diameter into nanoscale, novel optical properties may be observed [19]. The photoluminescence (PL) spectrum of synthesized antimony sulfide, shown in Figure 4a, b has an excitation peak at 390 nm (Figure 4a), and the emission peak can be observed at 420, 480nm (Figure 4b). This PL emission indicates a blue-shift phenomenon, as commonly observed for nanomaterials (band gap is 2.50 eV). The UV/Vis spectrum (prepared by dispersion of  $\text{Sb}_2\text{S}_3$  products in ethanol) shows an intense absorption band at 250 nm and broad band at 280nm (Figure 5).

## 4. CONCLUSIONS

In summary, a red-ox reaction approach in hydrothermal condition has been developed to prepare  $\text{Sb}_2\text{S}_3$  nanorods with high yield at 180°C and 24h. The length of nanorods is up to 3  $\mu\text{m}$  and their diameter is around 250-380 nm. Single crystals and crystal growth can be obtained by increasing the heating time up to 3 days. Using iodine as an initiator of oxidation reduction reaction is reported for the first time. The formation mechanism of  $\text{Sb}_2\text{S}_3$  based on red-ox reaction is proposed. In current process,  $\text{I}_2$  plays an important role in the formation of  $\text{Sb}_2\text{S}_3$  nanostructure, though other oxidizing agent can be worthwhile for preparing nanostructures in the future. Moreover, as a common feature for nanomaterials, a blue shift was observed in the case of optical absorption.

## 5. ACKNOWLEDGMENT

We are grateful to Research Council of university of Tabriz for the financial support of this research.

## REFERENCES

1. B. Roy, B. R. Chakraborty, R. Bhattacharya, A.K. Dutta, Solid. State. Commun. Vol. 25, (1978), pp. 937.
2. S.K. Srivastava, M. Pramanik, D. Palit, H. Haueseler, Chem. Mater. Vol. 16, (2004), pp. 4168.
3. O. Savadogo, K.C. Mandal, Energy Mater. Sol. Cells. Vol. 26, (1992), pp. 117.
4. B.H. Juarez, M. Ibizate, J.M. Palacios, C. Lopez, Adv. Mater. Vol. 15, (2003), pp. 319.
5. N.K. Abrikosov, V.F. Bankina, L.V. Poretakaya, L.E. Shelimova, Semiconducting II-VI and V-VI Compounds, Plenum, New York, 1969.
6. D. Arivuoli, F.D. Gnanam, P. Ramasamy, J. Mater. Sci. Lett. Vol. 7, (1988), pp. 711.

7. C. N. Rao, F. L. Deepak, G. Gundiah, *Prog. Solid State. Chem.* Vol. 31, (2003), pp. 5.
8. Z. R. Geng, M.X.Wang, G. H. Yue, P. X. Yan, *J. Cryst. Growth.* Vol. 10, (2008), pp. 341.
9. S. R. Messina, M. T. Nair, P. K. Nair, *Thin Solid Films.* Vol. 517, (2009), pp. 2503.
10. H. M. Yang, X. H. Su, A. D. Tang, *Mater. Res. Bull.* Vol. 42, (2007), pp. 1357.
11. M. Lallakantouri, A. G. Marison, G. E. Manoussakis, *J. Therm. Anal.* Vol. 29, (1984), pp. 1151.
12. J. Yang, H. Zeng, S. H. Yu, L. Yang, Y. H. Zhang, *Chem. Mater.* Vol. 12, (2000), pp. 2924.
13. W. J. Lou, M. Chen, X. B. Wang, W. M. Liu, *Chem. Mater.* Vol. 19, (2007), pp. 872.
14. Y. Yu, R. H. Wang, Q. Chen, L. M. Peng, *J. Phys. Chem.* Vol. B109, (2005), pp. 23312.
15. C. Li, X. G. Yang, Y. F. Liu, Z. Y. Zhao, Y. T. Qian, *J. Cryst. Growth.* Vol. 255, (2003), pp. 342.
16. X. Zheng, Y. Xie, L. Zhu, X. Jiang, Y. Jia, W. Song, *Inorg. Chem.* Vol. 41, (2002), pp. 455.
17. Y. T. Qian, K. Tang, C. Wang, G. Zhou, *J. Mater. Chem.* Vol. 11, (2001), pp. 257.
18. X. Wang, J. Zhang, Q. Peng, Y. Li, *Nature.* Vol. 437, (2005), pp. 121.
19. A. M. Qin, U. P. Fang, W. X. Zhao, *J. Cryst. Growth.* Vol. 283, (2005), pp. 230.

